PHYSICAL REVIEW LETTERS

Nonlinear Theory for a Quantum Diode in a Dense Fermi Magnetoplasma

P. K. Shukla and B. Eliasson

Theoretische Physik IV, Ruhr-Universität Bochum, D-44780 Bochum, Germany
(Received 19 October 2007; published 22 January 2008)

We present a simple analytical nonlinear theory for quantum diodes in a dense Fermi magnetoplasma. By using the steady-state quantum hydrodynamical equations for a dense Fermi magnetoplasma, we derive coupled nonlinear Schödinger and Poisson equations. The latter are numerically solved to show the effects of the quantum statistical pressure, the quantum tunneling (or the quantum diffraction), and the external magnetic field strength on the potential and electron density profiles in a quantum diode at nanometer scales. It is found that the quantum statistical pressure introduces a lower bound on the steady electron flow in the quantum diode, while the quantum diffraction effect allows the electron tunneling at low flow speeds. The magnetic field acts as a barrier, and larger potentials are needed to drive currents through the quantum diode.

Studies of charged particle dynamics in a plasma-filled gap are of significant interest in vacuum microelectronics, cross-field devices, and high power diodes. The familiar one-dimensional Child-Langmuir (CL) law [1,2] gives the maximum steady-state current, $J_{CL} = (1/9\pi) \times (2e/m_e)^{1/2}\phi_0^{3/2}/d^2$, which can be transported across a cathode-anode gap of spacing d and the cathode-anode potential difference ϕ_0, where e is the magnitude of the electron charge and m_e is the electron mass. Although the limited CL current in a gap remains a fundamental quantity, there are obvious modifications of the CL law due to geometrical [3] and relativistic effects [4]. Furthermore, in the emerging fields of nanotechnology or nanoelectronics, tunneling microscopy and vacuum microelectronics, nano-triodes and nanogaps, and nanojunctions, one encounters interesting phenomena at scales ranging from sub-10 nm to hundreds of nm. On such microscopic scales, quantum effects (e.g., the electron tunneling) cannot be neglected. Quantum extension of the CL law has been presented by Lau *et al.* [5], by using a simple mean-field model that is based on the coupled Schrödinger and Poisson equations. The authors of Ref. [5] reported that the limiting current in a quantum diode may far exceed the classical CL value due to the electron tunneling effect. Further theoretical models for space-charge limited flows in an unmagnetized ultra-cold quantum plasma have been developed by Ang *et al.* [6–8] and Ang and Zhang [9].

In this Letter, we present for the first time a simple nonlinear theory for a quantum diode in a dense Fermi magnetoplasma, accounting for the quantum statistical electron pressure and quantum electron tunneling effects, as well as by invoking the appropriate boundary conditions for a quantum plasma diode. We consider the planar diode configuration, where an insulating homogeneous magnetic field $\hat{\mathbf{z}}B_0$, where $\hat{\mathbf{z}}$ is the unit vector along the z axis in a Cartesian coordinate system and B_0 is the magnetic field strength, is applied parallel to the cathode (located at $x = 0$) and anode (located at $x = d$) surfaces. We assume that

the characteristic rise time of the anode voltage to the steady value $\phi_0(x = d) = \phi_0$ is long in comparison with the electron gyroperiod. The electrons are emitted from the cathode with a finite speed, and are accelerated (by the electric field $= -\partial\phi/\partial x$) towards the anode where the Voltage applied is ϕ_0. The electron dynamics in the steady state is governed by the quantum hydrodynamic (QHD) equations (in the mean-field approximation [10–12]), which are composed of the electron continuity equation

$$\frac{\partial(nv_x)}{\partial x} = 0, \tag{1}$$

the x and y components of the electron momentum equation

$$\frac{m_e}{2}\frac{\partial v_x^2}{\partial x} = e\left(\frac{\partial\phi}{\partial x} - \frac{1}{c}v_y B_0\right) + F_Q, \tag{2}$$

and

$$m_e v_x \frac{\partial v_y}{\partial x} = \frac{eB_0}{c}v_x, \tag{3}$$

respectively, and the Poisson equation

$$\frac{\partial^2\phi}{\partial x^2} = 4\pi en, \tag{4}$$

where $n = \psi^2$ is the macroscopic electron density, ψ is the modulus of the wave function of the electrons, v_x and v_y are the x and y components of the continuum electron fluid velocity, $E_x = -\partial\phi(x)/\partial x$ is the x component of the diode electric field, $\phi(x)$ is the scalar potential, k_B is the Boltzmann constant, $k_B T_{Fe} = (\hbar^2/2m_e)(3\pi^2)^{2/3}n_0^{2/3}$ is the Fermi electron temperature, $\hbar$ is the Planck constant divided by 2π, $n_0 = \psi_0^2$ is electron density at the anode ($x = 0$), and c is the speed of light in vacuum. Furthermore, the quantum force is

$$F_Q = -\frac{2k_B T_{Fe}}{3nn_0^2}\frac{\partial n^3}{\partial x} + \frac{\hbar^2}{2m_e}\frac{\partial}{\partial x}\left(\frac{1}{\sqrt{n}}\frac{\partial^2\sqrt{n}}{\partial x^2}\right), \tag{5}$$

where the first term on the right-hand side is derived from the quantum statistical pressure law [11,12] $p_e = (2m_e V_{\mathrm{Fe}}^2/3n_0^2)n^3$, where $V_{\mathrm{Fe}} = (k_B T_{\mathrm{Fe}}/m_e)^{1/2}$ is the Fermi electron thermal speed, and the second term is the quantum Bohm potential [10–12].

We note that Eqs. (1) and (3) are satisfied by, respectively,

$$nv_x = -J/e = \text{const}, \qquad (6)$$

and

$$v_y = \omega_{\mathrm{ce}}x, \qquad (7)$$

where $J < 0$ is the constant current and $\omega_{\mathrm{ce}} = eB_0/m_e c$ is the electron gyrofrequency. It should be noted that in the derivation of the CL law, the electrons are assumed to be emitted from the cathode with zero speed, which leads to a divergence of the electron density, while in reality the electrons are emitted from the cathode with a nonzero speed v_{0x}, and the electron density at the cathode is $n_0 = \psi_0^2$.

Inserting v_x and v_y from (6) and (7) into (2), we obtain an equation, which can be integrated once to obtain

$$\frac{\hbar^2}{2m_e^2}\frac{\partial^2\psi}{\partial x^2} + \left[\frac{e}{m_e}\phi + V_{\mathrm{Fe}}^2\left(1 - \frac{\psi^4}{\psi_0^4}\right)\right.$$
$$\left. + \frac{J^2}{2e^2\psi_0^4}\left(1 - \frac{\psi_0^4}{\psi^4}\right) - \omega_{\mathrm{ce}}^2\frac{x^2}{2}\right]\psi = 0, \quad (8)$$

while (4) takes the form

$$\frac{\partial^2\phi}{\partial x^2} = 4\pi e\psi^2. \qquad (9)$$

In deriving Eq. (8), we have imposed the boundary conditions $\partial^2\psi/\partial x^2 = 0$, $\psi = \psi_0$, and $\phi = 0$ at the cathode, which is located at $x = 0$. In what follows, we will also assume that $E = -\partial\phi/\partial x = 0$ and $\partial\psi/\partial x = 0$ at $x = 0$. We note that Eqs. (8) and (9) are solved exactly for $\psi = \psi_0$, $e\phi/m_e = \omega_{\mathrm{ce}}^2 x^2/2$, and $\omega_{\mathrm{ce}}^2 = \omega_{\mathrm{pe}}^2$ for any value of J. The Brillouin flow condition $\omega_{\mathrm{ce}}^2 = \omega_{\mathrm{pe}}^2$ also appears in the theory of magnetically isolated diodes (where $J = 0$) [4].

We note that by introducing the change of variable

$$\phi = \varphi + \frac{m_e\omega_{\mathrm{ce}}^2}{2e}x^2, \qquad (10)$$

the system of Eqs. (8) and (9) can be transformed to

$$\frac{\hbar^2}{2m_e^2}\frac{\partial^2\psi}{\partial x^2} + \left[\frac{e}{m_e}\varphi + V_{\mathrm{Fe}}^2\left(1 - \frac{\psi^4}{\psi_0^4}\right) + \frac{J^2}{2e^2\psi_0^4}\left(1 - \frac{\psi_0^4}{\psi^4}\right)\right]\psi = 0, \qquad (11)$$

and

$$\frac{\partial^2\varphi}{\partial x^2} = 4\pi e\left(\psi^2 - \frac{\omega_{\mathrm{ce}}^2}{\omega_{\mathrm{pe}}^2}\psi_0^2\right), \qquad (12)$$

respectively.

For the numerical treatment, it is convenient to rewrite the system (8) and (9) in a dimensionless form as

$$\frac{H^2}{2}\frac{\partial^2\Psi}{\partial X^2} + \left[\Phi + \tilde{V}_{\mathrm{Fe}}^2(1 - \Psi^4)\right.$$
$$\left. + \frac{\tilde{J}^2}{2}\left(1 - \frac{1}{\Psi^4}\right) - \frac{\omega_{\mathrm{ce}}^2}{\omega_{\mathrm{pe}}^2}\frac{X^2}{2}\right]\Psi = 0, \quad (13)$$

and

$$\frac{\partial^2\Phi}{\partial X^2} = \Psi^2, \qquad (14)$$

respectively. Here, $\Psi = \psi/\psi_0$, $\Phi = e\phi/m_e V_{\mathrm{Fe}}^2$, $X = \omega_{\mathrm{pe}}x/V_{\mathrm{Fe}}$, and $\omega_{\mathrm{pe}} = (4\pi\psi_0^2 e^2/m_e)^{1/2}$ is the electron plasma frequency. We have denoted the dimensionless current $\tilde{J} = J/e\psi_0^2 V_{\mathrm{Fe}}$, the quantum parameter $H = \hbar\omega_{\mathrm{pe}}/k_B T_{\mathrm{Fe}}$, and the normalized Fermi thermal speed $\tilde{V}_{\mathrm{Fe}}$. In our numerical simulation below, $\tilde{V}_{\mathrm{Fe}}$ is set to zero (one) to exclude (include) the quantum pressure effect, and $\tilde{J}$, H, and $\omega_{\mathrm{ce}}/\omega_{\mathrm{pe}}$ are set to different values to investigate the effects of flow speeds, quantum diffraction, and the magnetic field on the diode properties. To neglect the quantum diffraction effect, we set $H = 0$, and for the unmagnetized case, we set $\omega_{\mathrm{ce}}/\omega_{\mathrm{pe}} = 0$. The system of Eqs. (13) and (14) are then integrated with a fourth-order Runge-Kutta method with the appropriate boundary conditions at $X = 0$, and the integration ends at the anode at $X = d$. For the case $H = 0$, Eq. (13) is solved analytically for Ψ and inserted into (14), which is integrated numerically.

We first investigate Eqs. (8) and (9) for the classical and unmagnetized case $\hbar = V_{\mathrm{Fe}} = 0$ and $\omega_{\mathrm{ce}} = 0$. Here, we have from Eq. (8) $\psi^2 = \psi^2/\sqrt{1 + \beta\phi}$, where $\beta = 2e^3\psi_0^4/J^2 m_e$, which can be inserted into Eq. (9) to obtain

$$\frac{\partial^2\phi}{\partial x^2} = \frac{4\pi e\psi_0^2}{\sqrt{1 + \beta\phi}}. \qquad (15)$$

Multiplying the above equation by $\partial\phi/\partial x$ and integrating once, we obtain

$$\frac{1}{2}\left(\frac{\partial\phi}{\partial x}\right)^2 = \frac{8\pi e\psi_0^2}{\beta}\left(\sqrt{1 + \beta\phi} - 1\right), \qquad (16)$$
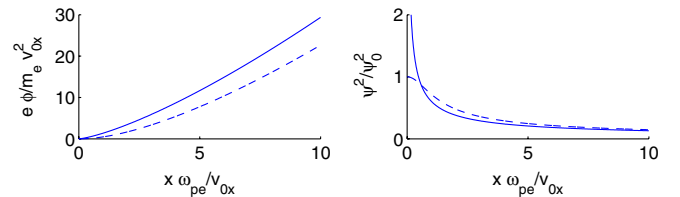
FIG. 1 (color online). The profiles of the electrostatic potential (left panel) and the electron density (right panel) for an unmagnetized classical diode ($\omega_{\mathrm{ce}} = \hbar = V_{\mathrm{Fe}} = 0$) with $J = -ev_{0z}\psi_0^2$. The dashed lines shows the exact solution, and the solid line shows the Child-Langmuir law.
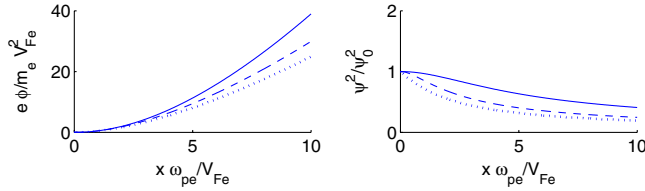
FIG. 2 (color online). The profiles of the electrostatic potential (left panel) and the electron density (right panel) for an unmagnetized diode ($\omega_{ce} = 0$), where we have neglected the quantum diffraction effect ($\hbar = 0$). The currents are $J = -ev_{x0}\psi_0^2$, with terminal speeds $v_{x0} = 4V_{Fe}$ (solid lines), $v_{x0} = 2V_{Fe}$ (dashed lines), and $v_{x0} = \sqrt{2}V_{Fe}$ (dotted lines). The latter case corresponds to the lower speed limit for a well-defined quantum diode.

where we used the boundary conditions $\phi = \partial\phi/\partial x = 0$ at $x = 0$. Introducing the new variable $\chi = \sqrt{\sqrt{1 + \beta\phi} - 1}$, the equation above can readily be integrated once more to obtain [2]

$$\chi^3 + 3\chi = \frac{3x}{2}\sqrt{4\pi e\psi_0^2 \beta}, \qquad (17)$$

which relates ϕ to x. In the limiting case $\beta\phi \gg 1$, we have $\chi \approx (\beta\phi)^{1/4}$, which, by using (12), yields $(\beta\phi)^{3/4} = (3x/2)\sqrt{4\pi e\psi_0^2 \beta}$, and we recover the classical Child-Langmuir law [4]

$$\phi = \left(9\pi\sqrt{\frac{m}{2e}}|J|\right)^{2/3} x^{4/3}. \qquad (18)$$

In Fig. 1, we have plotted the exact solution as well as the Child-Langmuir law. For the Child-Langmuir law, the density formally goes to infinity at $x = 0$, while with appropriate boundary conditions, we have a finite density at $x = 0$.

Next, we investigate the influence of the quantum statistical pressure on the unmagnetized diode. It turns out that there exist a quantum Bohm criterion for the existence of a well-defined steady-state stream of electrons charac-
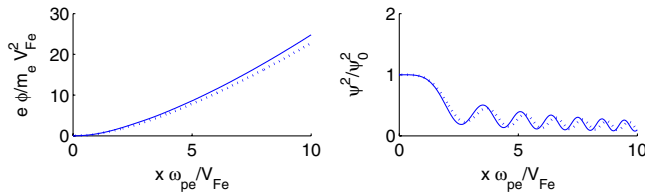
FIG. 3 (color online). The profiles of the electrostatic potential (left panels) and the electron density (right panels) for an unmagnetized diode for the case where we have neglected the quantum statistical pressure effect (dotted lines) and for the case where it has been included (solid lines). We use to $H = 2$ and $J = -1.0 \times e\psi_0^2 V_{Fe}$ (i.e., $v_{x0} = V_{Fe}$); even though the Bohm criterion is violated, electrons can tunnel through the diode due to the quantum tunneling effect.
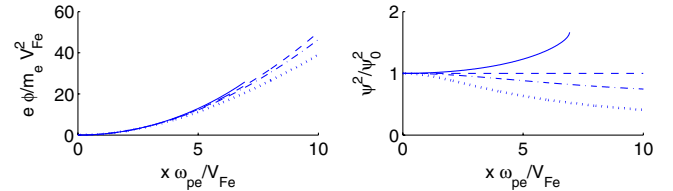
FIG. 4 (color online). The profiles of the electrostatic potential (left panel) and the electron density (right panel) for a magnetized diode where we have neglected the quantum diffraction effect ($\hbar = 0$). We used $J = -4e\psi_0 V_{Fe}$ and $\omega_{ce} = 0$ (dotted lines), $\omega_{ce} = 0.9\omega_{pe}$ (dash-dotted lines), $\omega_{ce} = \omega_{pe}$ (dashed lines), and $\omega_{ce} = 1.1\omega_{pe}$ (solid lines). The diode has a maximum critical width for $\omega_{ce}/\omega_{pe} > 1$.

terized by a decreasing density and positive potential. Linearizing Eq. (8) as $\psi = \psi_0 + \psi_1$, $|\psi_1| \ll \psi_0$ and $\phi = \phi_1$ with the Bohm potential term equal to zero, we find that $e\phi_1/m_e = 4(V_{Fe}^2 - J^2/2e^2\psi_0^4)\psi_1/\psi_0$. By requiring that negative ψ_1 should give rise to positive ϕ_1, we find the condition $J^2 > 2e^2\psi_0^4 V_{Fe}^2$. By using the relation $J = -ev_{x0}\psi_0^2$, where v_{x0} is the terminal speed at $x = 0$, we find the "quantum Bohm criterion" $v_{x0} > \sqrt{2}V_{Fe}$. In Fig. 2, we have plotted the profiles and electron densities for several values of v_{x0}, including the limiting case $v_{x0} = \sqrt{2}V_{Fe}$. Larger values of v_{x0} are correlated with larger potentials and higher electron densities. Hence, in our quantum fluid picture, there exist a minimum critical potential ϕ_c, as a function of V_{Fe} and d, for the development of a steady-state electron flow. If the electron diffraction effect is included, the current is allowed to take values
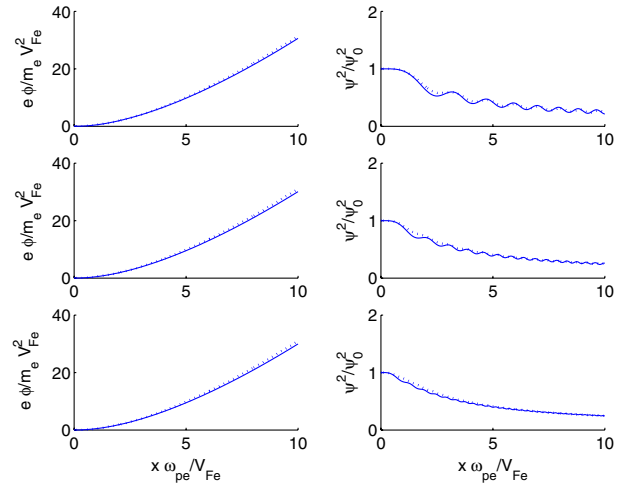
FIG. 5 (color online). The profiles of the electrostatic potential (left panels) and the electron density (right panels) for an unmagnetized diode, for the case where we have neglected the quantum statistical pressure effect (dotted lines) and for the case where it has been included (solid lines). The quantum parameter is $H = 2$, $H = 1$, and $H = 0.5$ (top to bottom panels). We use $J = -2.0e\psi_0^2 V_{Fe}$ (i.e., $v_{x0} = 2V_{Fe}$), so that the Bohm criterion is fulfilled.
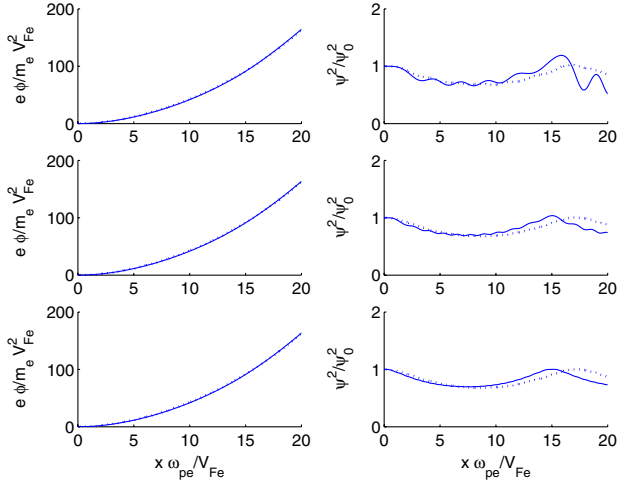
FIG. 6 (color online).   The profiles of the electrostatic potential (left panels) and the electron density (right panels) for a magnetized quantum diode with $\omega_{ce}/\omega_{pe} = 0.9$, for the case where we have neglected the quantum statistical pressure (dotted lines) and for the case where it has been included (solid lines). The quantum parameter is $H = 2$, $H = 1$, and $H = 0.5$ (top to bottom panels). We use $J = -2.0 \times e\psi_0^2 V_{Fe}$ (i.e., $v_{x0} = V_{Fe}$), so that the Bohm criterion is fulfilled for the case where the quantum pressure is included. We see that the electron density profile exhibits a second maximum at $x \approx 15V_{Fe}/\omega_{pe}$, and for larger values of x (not shown here), similar maxima appear in a quasiperiodic manner.

below the quantum Bohm limit. This is illustrated in Fig. 3, where we have used the flow speed $v_{x0} = V_{Fe}$. We see in Fig. 3 that the electron density shows an oscillatory behavior due to the quantum diffraction effect.

The influence of the magnetic field on the diode is illustrated in Fig. 4, where we have plotted the potential and the electron density for different values of ω_{ce}/ω_{pe}. For $\omega_{ce}/\omega_{pe} = 0$, we have the unmagnetized case with a monotonically increasing potential driving a monotonically decreasing electron density. Larger values of ω_{ce}/ω_{pe} give larger potentials and higher electron densities. For $\omega_{ce}/\omega_{pe} = 1$, we have the limiting case of the Brillouin flow with constant density. For $\omega_{ce}/\omega_{pe} > 1$, the electron density is increasing for a positive potential, and the steady-state solution has a critical maximum width; in our case, for $\omega_{ce}/\omega_{pe} = 1.1$, the critical width is $x \approx 7V_{Fe}/\omega_{pe}$. For larger x-values than shown in Fig. 4, we have seen that for finite $\omega_{ce}/\omega_{pe} < 1$, the electron density becomes nonmonotonic, and exhibits a periodic behavior (similarly as shown in Fig. 6 below).

In Fig. 5, we have investigated the effects of the quantum statistical pressure and quantum tunneling on an unmagnetized diode, for a larger current and larger potential than those in Fig. 3. The impact of the quantum statistical

pressure on the potential and the electron density is only minor, while larger values of H lead to visible oscillations in the electron density. For the magnetized case, shown in Fig. 6, the potential is somewhat higher (e.g., at $x = 10V_{Fe}/\omega_{pe}$), and the electron densities are significantly higher for the same current as in Fig. 5. We see in Fig. 6 that the electron density is nonmonotonic and exhibits a maximum at $x \approx 15V_{Fe}/\omega_{pe}$, and for larger values of x (not shown here), the electron density has a quasiperiodic behavior.

To summarize, we have developed a nonlinear model for a quantum diode in a dense Fermi magnetoplasma, taking into account the quantum statistical pressure law for the electrons, and the quantum Bohm potential that causes the electron tunneling. In the absence of the latter, the quantum statistical pressure law leads to a lower speed limit at $x = 0$, similar to the Bohm criterion for the plasma sheath [13], below which the steady-state electron flow ceases to exist. However, the quantum tunneling effect may lower this speed limit. Furthermore, the external magnetic field acts as a barrier on the electron flow, so that a larger potential is needed to drive the current in magnetized quantum diodes at nanometer scales.

[1] C. D. Child, Phys. Rev. (Series I) **32**, 492 (1911); I. Langmuir, Phys. Rev. **21**, 419 (1923).
[2] G. Jaffe, Phys. Rev. **65**, 91 (1944).
[3] J. W. Luginsland, Y. Y. Lau, and R. M. Gilgenbach, Phys. Rev. Lett. **77**, 4668 (1996); Y. Y. Lau, *ibid.* **87**, 278301 (2001).
[4] R. C. Davidson, *Physics of Nonneutral Plasmas* (Addison-Wesley, Redwood City, CA, 1999), Chap. 8, pp. 461.
[5] Y. Y. Lau *et al.*, Phys. Rev. Lett. **66**, 1446 (1991).
[6] L. K. Ang, T. J. T. Kwan, and Y. Y. Lau, Phys. Rev. Lett. **91**, 208303 (2003).
[7] L. K. Ang, Y. Y. Lau, and T. J. T. Kwan, IEEE Trans. Plasma Sci. **32**, 410 (2004).
[8] L. K. Ang, W. S. Koh, Y. Y. Lau, and T. J. T. Kwan, Phys. Plasmas **13**, 056701 (2006).
[9] L. K. Ang and P. Zhang, Phys. Rev. Lett. **98**, 164802 (2007).
[10] C. L. Gardner and C. Ringhofer, Phys. Rev. E **53**, 157 (1996).
[11] G. Manfredi and F. Haas, Phys. Rev. B **64**, 075316 (2001); G. Manfredi, Fields Inst. Commun. **46**, 263 (2005).
[12] F. Haas, Phys. Plasmas **12**, 062117 (2005).
[13] D. Bohm, in *The Characteristics of Electrical Discharges in Magnetic Field*, edited by A. Guthrie and R. K. Wakerling (McGraw-Hill, New York, 1949), Chap. 3; D. Lee *et al.*, Phys. Rev. Lett. **99**, 155004 (2007).